Article:
De Reggi, S., Scarabel, F. and Vermiglio, R. (Accepted: 2026) On The Convergence Of The Pseudospectral Approximation Of Reproduction Numbers For Age-Structured Models. SIAM Journal on Numerical Analysis. ISSN: 0036-1429 (In Press)

ON THE CONVERGENCE OF THE PSEUDOSPECTRAL APPROXIMATION OF REPRODUCTION NUMBERS FOR AGE-STRUCTURED MODELS *

SIMONE DE REGGI[§ †], FRANCESCA SCARABEL[§ ‡], AND ROSSANA VERMIGLIO[§]

Abstract. We rigorously investigate the convergence of a new numerical method, recently proposed by the authors, to approximate the reproduction numbers of a large class of age-structured population models with finite age span. The method consists in reformulating the problem in a space of absolutely continuous functions via an integral mapping. For any chosen splitting into birth and transition processes, we first define an operator that maps a generation to the next one (corresponding to the Next Generation Operator in the case of R_0). Then, we approximate the infinite-dimensional operator with a matrix using pseudospectral discretization. In this paper, we prove that the spectral radius of the resulting matrix converges to the true reproduction number, and the (interpolation of the) corresponding eigenvector converges to the associated eigenfunction, with convergence order that depends on the regularity of the model coefficients. Results are confirmed experimentally and applications to epidemiology are discussed.

Key words. Basic reproduction number, error bounds, next generation operator, pseudospectral collocation, spectral approximation, spectral radius.

MSC codes. 34L16, 47B07, 65L15, 65L60, 65N12, 92D25

1. Introduction. Age-structured population models are often formulated as integro-partial differential equations with nonlocal boundary conditions. As a result, they generate infinite-dimensional dynamical systems where, typically, the state space X is a space of L^1-integrable functions over the age-interval $(0, a^\dagger)$, where $a^\dagger \in (0, +\infty]$ is the maximum age. Such models have applications in many fields in the life sciences, including ecology, epidemiology, and cell biology [24, 27, 46]. In all these contexts, *reproduction numbers* play a fundamental role, as they describe the number of new individuals generated by one typical individual in the population (details about the interpretation of "new" and "typical" individual will depend on the context). Because of this interpretation, they are threshold parameters that determine population/disease persistence or extinction, and can be linked to intervention measures for population/disease control [32]. Mathematically, they are characterized as the spectral radius of linear, compact, positive operators [16, 27, 40], which can be obtained by linearizing the model around an equilibrium and then splitting the linearization into *birth* and *transition* [3, 17, 45]. The resulting operators are typi-

*Accepted for publication

Funding: The authors are members of the INdAM Research group GNCS and UMI Research group "Modellistica socio-epidemiologica". FS is a member of JUNIPER (Joint UNIversities Pandemic and Epidemiological Research). The work of SDR and RV was supported by the Italian Ministry of University and Research (MUR) through the PRIN 2020 project (No. 2020JLWP23) "Integrated Mathematical Approaches to Socio-Epidemiological Dynamics", Unit of Udine (CUP: G25F22000430006). SDR was partially supported by the project "One Health Basic and Translational Actions Addressing Unmet Needs on Emerging Infectious Diseases" (INF-ACT), BaC "Behaviour and sentiment monitoring and modelling for outbreak control/BEHAVE-MOD" (No. PE00000007 – CUP I83C22001810007) funded by the NextGenerationEU. The work of FS was partially supported by the Engineering and Physical Sciences Research Council grant UKRI170: "The dynamics of waning and boosting of immunity: new modelling and numerical tools" and by the University of Leeds REDI Pilot Fund.

†Department of Mathematics, University of Trento, Italy (simone.dereggi@unitn.it).

‡School of Mathematics, University of Leeds, United Kingdom (f.scarabel@leeds.ac.uk).

§CDLab - Computational Dynamics Laboratory, Department of Mathematics, Computer Science and Physics, University of Udine, Italy (rossana.vermiglio@uniud.it).

cally infinite-dimensional, which makes the computation of the reproduction numbers hardly analytically achievable, in general.

Several numerical methods have been proposed to approximate the reproduction numbers for age-structured models with finite age span, i.e., with $a^\dagger < +\infty$ [5, 6, 7, 22, 31]. Their core idea is to separately discretize the birth and transition operators, and then approximate the corresponding reproduction number through the spectral radius of a matrix. The discretization is obtained via Theta method [22], Backward Euler method [31], and Chebyshev pseudospectral collocation [5, 6, 7]. However, all these methods rely on the assumption that the birth and transition operators are defined on a subspace of the state space X, including the boundary conditions in the domain of the transition operator (which in general is a differential operator), hence necessarily interpreting the corresponding processes as transition.

To overcome this lack of flexibility, in [15] we introduced a general numerical method to approximate the reproduction numbers for a large class of age-structured models with finite age span, by reformulating the problem in a space of absolutely continuous (AC) functions via integration of the age-state, within the extended space framework [25, 27, 40]. On the one hand, this approach permits us to interpret processes described by boundary conditions as perturbations of an operator with trivial domain condition and, on the other hand, it allows us to work with polynomial interpolation, since point evaluation is well-defined. For any given splitting into birth and transition, we discretize the resulting operators via Chebyshev pseudospectral collocation.

In this paper, we rigorously investigate the convergence of the method presented in [15]. To do so, we use the well-established spectral approximation theory of [12]. To prove the norm convergence of the operators in AC, we take advantage of the injection of AC into L^1, which is compact by the Rellich–Kondrachov Theorem [11, p. 285, Theorem 9.16], and of interpolation error bounds in the L^1-norm [35, Theorem 1]. Note that this approach is not common in the literature as, typically, the convergence of spectral and pseudospectral methods is investigated in the supremum norm for continuous functions, or in Hilbert spaces [4]. We prove that the convergence order of the approximating reproduction numbers is driven by the interpolation error of the relevant (generalized) eigenfunctions, which in turn depends on the regularity of the model coefficients. We discuss applications to epidemiological models, which can require to work with piecewise constant coefficients in the case of data-informed parameters.

The paper is organized as follows. In section 2, with reference to the prototype linear model considered in [15], we illustrate the reformulation in AC together with the theoretical framework. In section 3, we recall the numerical method of [15] and we prove the well-posedness of the discretized operator. The main contribution of the paper is the convergence proof in section 4. In section 5, we give details about the implementation of the method, while section 6 contains numerical results and applications to epidemiological models.

MATLAB demos are available at http://cdlab.uniud.it/software.

2. Prototype model and theoretical background. In this section, we make reference to the prototype linear age-structured population model with finite age span considered in [15], which includes, as particular instances, many models of the literature obtained from the linearization of nonlinear models around an equilibrium. For $a^\dagger \in (0, +\infty)$, $x(t, \cdot) \in X := L^1([0, a^\dagger], \mathbb{R}^d)$, $t \geq 0$ and d a positive integer, the model reads

$$\begin{cases} \mathcal{D}x(t,a) = \int_0^{a^\dagger} \beta(a,\alpha)x(t,\alpha)\,\mathrm{d}\alpha + \delta(a)x(t,a), & t \geq 0,\ a \in [0,a^\dagger], \\ x(t,0) = \int_0^{a^\dagger} b(a)x(t,a)\,\mathrm{d}a, & t \geq 0, \end{cases} \tag{2.1}$$

where

$$\mathcal{D}x(t,a) \coloneqq \partial_t x(t,a) + \partial_a x(t,a).$$

To conveniently split the inflow processes into two parts, we assume that $\beta = \beta^+ + \beta^-$ and $b = b^+ + b^-$, where $\beta^+, \beta^-, b^+, b^-, \delta$ satisfy the following requirements, motivated by applications to epidemiology and demography [27, p. 77].

Assumption 1.
- (*i*) *$\beta^+, \beta^- \in L^\infty([0,a^\dagger]^2, \mathbb{R}^{d\times d})$ and $b^+, b^- \in L^\infty([0,a^\dagger], \mathbb{R}^{d\times d})$ are all nonnegative,*
- (*ii*) *$\delta \in L^\infty([0,a^\dagger], \mathbb{R}^{d\times d})$ is Metzler (i.e., all its off-diagonal entries are nonnegative) with nonpositive diagonal elements.*

Note that Assumption 1 (*ii*) ensures that the fundamental solution matrix associated to δ is nonnegative and nonsingular [27, p. 77]. Together with (*i*), this implies that for every nonnegative initial condition $x(0,\cdot) = \phi_0 \in X$, system (2.1) admits a unique nonnegative solution, see [27, Chapters 1 and 2] and [20, Sections III.1 and VI.1.b]. In this case, for all $t \geq 0$, $(x(t,\cdot))_j$ is the population age-density over the interval $[0,a^\dagger]$ of group $j = 1,\dots,d$.

We consider the Banach space $Y \coloneqq AC([0,a^\dagger], \mathbb{R}^d)$ equipped with the norm $\|\psi\|_Y \coloneqq |\psi(0)|_{\mathbb{R}^d} + \|\psi'\|_X$. The Volterra operator $\mathcal{V}_0 \colon X \to Y_0 \subset Y$ defined as

$$(\mathcal{V}_0\phi)(a) \coloneqq \int_0^a \phi(\alpha)\,\mathrm{d}\alpha, \quad a \in [0,a^\dagger],$$

is an isomorphism between X and the closed subspace $Y_0 \coloneqq \{\psi \in Y \mid \psi(0) = 0\} \subset Y$.

By defining $y(t,\cdot) \coloneqq \mathcal{V}_0 x(t,\cdot)$, system (2.1) is equivalent to

$$\begin{cases} \mathcal{D}y(t,a) = \int_0^{a^\dagger} b(\alpha)y(t,\mathrm{d}\alpha) \\ \qquad\qquad + \int_0^a \int_0^{a^\dagger} \beta(\zeta,\alpha)y(t,\mathrm{d}\alpha)\,\mathrm{d}\zeta \\ \qquad\qquad + \int_0^a \delta(\alpha)y(t,\mathrm{d}\alpha), & t \geq 0, \quad a \in [0,a^\dagger], \\ y(t,0) = 0, & t \geq 0. \end{cases} \tag{2.2}$$

Note that, in (2.2), we interpret a function in AC as a measure. The element $(y(t,a))_j$ is the cumulative number of individuals with age in $[0,a]$ in group $j = 1,\dots,d$. Since $x(t,\cdot)$ is nonnegative, $y(t,\cdot)$ belongs to the cone $C \subset Y$ defined by

$$C \coloneqq \{\psi \in Y \mid \psi \geq 0 \text{ and } \psi \text{ is nondecreasing}\}. \tag{2.3}$$

Now, we define a bounded linear operator $\mathcal{B} \colon Y \to Y$ accounting for birth

$$(\mathcal{B}\psi)(a) \coloneqq \int_0^a \int_0^{a^\dagger} \beta^+(\zeta,\alpha)\psi'(\alpha)\,\mathrm{d}\alpha\,\mathrm{d}\zeta + \int_0^{a^\dagger} b^+(\alpha)\psi'(\alpha)\,\mathrm{d}\alpha, \qquad a \in [0,a^\dagger],$$

and an unbounded linear operator $\mathcal{M}\colon D(\mathcal{M}) \subset Y_0 \to Y$ accounting for transition

$$\begin{aligned}(\mathcal{M}\psi)(a) &\coloneqq \psi'(a) - \int_0^a \delta(\alpha)\psi'(\alpha)\,\mathrm{d}\alpha \\ &\quad - \int_0^a \int_0^{a^\dagger} \beta^-(\zeta,\alpha)\psi'(\alpha)\,\mathrm{d}\alpha\,\mathrm{d}\zeta - \int_0^{a^\dagger} b^-(\alpha)\psi'(\alpha)\,\mathrm{d}\alpha, \qquad a \in [0,a^\dagger], \\ D(\mathcal{M}) &\coloneqq \{\psi \in Y_0 \mid \psi' \in Y\}.\end{aligned}$$

We also define the baseline transition operator $\mathcal{M}_0\colon D(\mathcal{M}) \to Y$ as

$$(\mathcal{M}_0\psi)(a) \coloneqq \psi'(a) - \int_0^a \delta(\alpha)\psi'(\alpha)\,\mathrm{d}\alpha, \qquad a \in [0,a^\dagger],$$

which, under Assumption 1 (ii), is invertible with bounded inverse. Observe that the operator $\mathcal{B}_- \coloneqq \mathcal{M}_0 - \mathcal{M}$ contains the inflow processes described by β^- and b^- and, under Assumption 1 (i), $\mathcal{B}_-\mathcal{M}_0^{-1}\colon Y \to Y$ is bounded. From a biological point of view, we want to ensure that the inflow processes contained in β^-, b^- alone cannot sustain the population/epidemic growth. Mathematically, this is guaranteed by the following assumption.

Assumption 2. *$\rho(\mathcal{B}_-\mathcal{M}_0^{-1}) < 1$, where ρ denotes the spectral radius.*

This condition also implies that $\mathcal{M}$ is invertible with bounded inverse, indeed [26]

$$\mathcal{M}^{-1} = \mathcal{M}_0^{-1}(\mathcal{I}_Y - \mathcal{B}_-\mathcal{M}_0^{-1})^{-1}, \tag{2.4}$$

where $\mathcal{I}_Y$ is the identity operator in Y. Hence, we can define the operator

$$\mathcal{H} \coloneqq \mathcal{B}\mathcal{M}^{-1}\colon Y \to Y, \tag{2.5}$$

and characterize the *reproduction number* R for the birth process $\mathcal{B}$ and transition process $\mathcal{M}$ as [15, 16]

$$R \coloneqq \rho(\mathcal{H}). \tag{2.6}$$

Here, we generically refer to "reproduction number" to account for several different interpretations, including, as special cases, the basic reproduction number R_0 and the type reproduction number T, as well as more general definitions [44, 23, 27]. Note that in (2.5), the operator $\mathcal{B}$ actually acts on $D(\mathcal{M})$.

To conclude this section, we prove that the operator $\mathcal{H}$ in (2.5) is compact in Y, and that R is a real dominant eigenvalue (in the sense of largest in magnitude). To do so, we consider the operator $\mathcal{W}\colon X \to Y \subset X$ defined as

$$\begin{aligned}(\mathcal{W}\phi)(a) \coloneqq &\int_0^a \delta(\alpha)\phi(\alpha)\,\mathrm{d}\alpha \\ &+ \int_0^a \int_0^{a^\dagger} \beta^-(\zeta,\alpha)\phi(\alpha)\,\mathrm{d}\alpha\,\mathrm{d}\zeta \\ &+ \int_0^{a^\dagger} b^-(\alpha)\phi(\alpha)\,\mathrm{d}\alpha, \qquad a \in [0,a^\dagger],\end{aligned}$$

and the natural immersion of Y into X, $\mathcal{J}\colon Y \to X$, which is compact due to the Rellich–Kondrachov embedding Theorem [11, p. 285, Theorem 9.16]. Note that, thanks to this, the restriction to Y of a linear and bounded operator from X to Y is compact. In the following, to simplify the notation, we omit to write $\mathcal{J}$ when the domain of application is clear from the context.

For all $\phi \in Y$ and $\psi = \mathcal{V}_0\phi \in D(\mathcal{M})$, we have

$$(\mathcal{I}_Y - \mathcal{W})\phi = \mathcal{M}\mathcal{V}_0\phi = \mathcal{M}\psi \in Y. \tag{2.7}$$

From (2.7) and Assumption 2 it follows that the operator $\mathcal{I}_Y - \mathcal{W} \colon Y \to Y$ is invertible with bounded inverse. Moreover, we can prove the following result that will be widely used later on in the paper.

Lemma 2.1. *The operator*

$$\mathcal{I}_X - \mathcal{W} \colon X \to X$$

is invertible with bounded inverse. Moreover, we have

$$\mathcal{M}^{-1} = \mathcal{V}_0 \left(\mathcal{I}_X - \mathcal{W}\right)^{-1} \mathcal{J}, \tag{2.8}$$

and the following inequality holds

$$\|\mathcal{M}^{-1}\|_{Y_0 \leftarrow Y} \leq a^\dagger \cdot \|(\mathcal{I}_X - \mathcal{W})^{-1}\|_{X \leftarrow X}. \tag{2.9}$$

Proof. Observe that $\mathcal{W}$ is compact in X. Thus, to prove the invertibility of $\mathcal{I}_X - \mathcal{W}$, we only need to show that there exists no $\phi \in X \setminus \{0\}$ such that $\phi = \mathcal{W}\phi$. Suppose in fact that $\phi \in X$ solves $\phi = \mathcal{W}\phi$. Then, $\phi \in Y$ and the invertibility of $\mathcal{I}_Y - \mathcal{W}$ in Y implies that $\phi = 0$.

Now, for $\xi \in Y$, solving $\mathcal{M}\psi = \xi$ in Y for $\psi = \mathcal{V}_0\psi'$ is equivalent to solve

$$\psi' - \mathcal{W}\psi' = \mathcal{J}\xi$$

in X for $\psi' \in Y$, hence (2.8) holds. Finally, the bound (2.9) follows from (2.8) by observing that $\|\mathcal{V}_0\|_{Y_0 \leftarrow X} = 1$ and that

$$\|\mathcal{J}\xi\|_X \leq a^\dagger \|\xi\|_Y, \qquad \xi \in Y. \tag{2.10}$$

□

From Lemma 2.1, we have that the following diagram commutes

$$\begin{tikzcd} Y \arrow[r, "\mathcal{M}^{-1}"] \arrow[d, "\mathcal{J}"'] & Y_0 \\ X \arrow[r, "(\mathcal{I}_X - \mathcal{W})^{-1}"'] & X \arrow[u, "\mathcal{V}_0"'] \end{tikzcd}$$

and, from the compactness of $\mathcal{J}$, we immediately get the following result.

Corollary 2.2. *The operator $\mathcal{H}$ in (2.5) is compact, $0 \in \sigma(\mathcal{H})$ and $\sigma(\mathcal{H}) \setminus \{0\}$ is a bounded set that consists only of eigenvalues with finite algebraic multiplicity, with no accumulation points except, possibly, for 0. In addition, if R in (2.6) is positive, then it is a real dominant eigenvalue with associated an eigenfunction $\psi \in C \setminus \{0\}$.*

Proof. Since $\mathcal{B}$ is bounded, it is enough to show that $\mathcal{M}^{-1}$ is compact. This follows by combining (2.8) with the compactness of $\mathcal{J}$. Then, the assertion on the spectrum of $\mathcal{H}$ follows from standard results on compact operators [29, Section 3.1 and p. 32, Theorem 3.11].

To prove the last claim, note that the cone C defined in (2.3) is total [27, Section 10.2], as $C \cap -C = \{0\}$ and, from standard results on bounded variation functions (see, e.g., [11, p. 206, Remark 8]), $C - C = Y$. Now, observe that, for all $\xi \in Y$,

$$\mathcal{M}_0^{-1}\xi = \mathcal{V}_0\left(U(\cdot,0)\xi(0) + \int_0^{\cdot} U(\cdot,\alpha)\xi'(\alpha)\,\mathrm{d}\alpha\right), \tag{2.11}$$

where $U(a,\alpha) \in \mathbb{R}^{d\times d}$, for $a,\alpha \in [0,a^\dagger]$, is the fundamental solution matrix associated to δ. Under Assumption 1 (ii), it is not difficult to see that (2.11) gives $\mathcal{M}_0^{-1}(C) \subset C$. Moreover, Assumption 2 ensures that [29, p. 149, Theorem 10.10]

$$\left(\mathcal{I}_Y - \mathcal{B}_-\mathcal{M}_0^{-1}\right)^{-1} = \sum_{k=0}^{+\infty}(\mathcal{B}_-\mathcal{M}_0^{-1})^k.$$

Thus, using Assumption 1 (i) and (2.4), one gets $\mathcal{H}(C) \subset C$. Finally, combining the compactness of $\mathcal{H}$ with the Krein–Rutman Theorem [28] (see also [27, p. 518, Theorem 10.8]), we conclude that, if $R > 0$, then it is a real dominant eigenvalue with associated an eigenfunction $\psi \in C \setminus \{0\}$. ∎

Remark 2.3. Assumption 1 is typical of applications to epidemiology and demography, and guarantees the positivity of solutions of (2.1). However, nonnegativity can be relaxed when considering other types of models, for instance coming from systems of interacting populations in ecology (see, e.g., [36] and references therein). In fact, all the previous and the following proofs remain valid as long as $\mathcal{M}^{-1}$ is invertible with bounded inverse, $\mathcal{M}^{-1}(C) \subset C$ and $\mathcal{B}(C) \subset C$ (hence $\mathcal{H}(C) \subset C$).

3. The numerical approach. To derive an approximation of R, we construct a finite-dimensional approximation $\mathcal{H}_N$ of $\mathcal{H}$, and we approximate the eigenvalues of the latter by those of the former. To do this, we separately discretize the operators $\mathcal{B}$ and $\mathcal{M}$ in section 2 via pseudospectral collocation [4, 41]. In the following, complexification is assumed everywhere as we deal with eigenvalues and eigenfunctions, and we adopt the MATLAB-like notation according to which elements of a column vector are separated by ";" while elements of a row vector are separated by ",".

3.1. Discretization of $\mathcal{B}$ and $\mathcal{M}$. Given a positive integer N, we consider the space $Y_N \subset Y$ of algebraic polynomials on $[0,a^\dagger]$ of degree at most N and taking values in $\mathbb{C}^d$, together with

$$Y_{0,N} \coloneqq \{\psi_N \in Y_N \mid \psi_N(0) = 0\} \subset Y_0.$$

Let $\Theta_N \coloneqq \{a_1 < \cdots < a_N\}$ denote a mesh of points in $(0,a^\dagger)$ and $\Theta_{0,N} \coloneqq \{a_0 = 0\} \cup \Theta_N$. We define restriction and prolongation operators respectively as

$$\mathcal{R}_N \colon Y \to \mathbb{C}^{dN}, \qquad \mathcal{R}_N\psi \coloneqq (\psi(a_1);\ldots;\psi(a_N)),$$

and

$$\mathcal{P}_{0,N} \colon \mathbb{C}^{dN} \to Y_{0,N}, \qquad \mathcal{P}_{0,N}\Psi \coloneqq \sum_{i=1}^{N} \ell_{0,i}\Psi_i,$$

where $\Psi := (\Psi_1; \ldots; \Psi_N)$, for $\Psi_i \in \mathbb{C}^d$, $i = 1, \ldots, N$, and $\{\ell_{0,i}\}_{i=0}^N$ is the Lagrange polynomial basis relevant to $\Theta_{0,N}$. Observe that

$$\mathcal{R}_N \mathcal{P}_{0,N} = \mathcal{I}_{\mathbb{C}^{dN}}, \qquad \mathcal{P}_{0,N} \mathcal{R}_N = \mathcal{L}_{0,N},$$

where $\mathcal{L}_{0,N} \colon Y_0 \to Y_{0,N}$ is the Lagrange interpolation operator relevant to $\Theta_{0,N}$.

Then, we derive the finite-dimensional approximations $\mathcal{B}_N, \mathcal{M}_N \colon \mathbb{C}^{dN} \to \mathbb{C}^{dN}$ of $\mathcal{B}$ and $\mathcal{M}$, respectively, as

$$\mathcal{B}_N := \mathcal{R}_N \mathcal{B} \mathcal{P}_{0,N}, \qquad \mathcal{M}_N := \mathcal{R}_N \mathcal{M} \mathcal{P}_{0,N}.$$

In order to derive a finite-dimensional approximation $\mathcal{H}_N$ of $\mathcal{H}$, in the next section we show that there exists a positive integer $\bar{N}$ such that $\mathcal{M}_N$ is invertible for every integer $N \geq \bar{N}$ under the following assumption.

Assumption 3. *Θ_N is the mesh of Chebyshev zeros [43].*

Subsequently, $\mathcal{H}_N \colon \mathbb{C}^{dN} \to \mathbb{C}^{dN}$ is defined as

$$\mathcal{H}_N := \mathcal{B}_N \mathcal{M}_N^{-1}, \qquad N \geq \bar{N}.$$

3.2. Invertibility of $\mathcal{M}_N$. We consider the Lagrange polynomial basis relevant to Θ_N, $\{\ell_i\}_{i=1}^N$, and define the prolongation operator

$$\mathcal{P}_{N-1} \colon \mathbb{C}^{dN} \to Y_{N-1} \subset Y, \qquad \mathcal{P}_{N-1}\Phi := \sum_{i=1}^N \ell_i \Phi_i,$$

where $\Phi := (\Phi_1; \ldots; \Phi_N)$. Note that

$$\mathcal{R}_N \mathcal{P}_{N-1} = \mathcal{I}_{\mathbb{C}^{dN}}, \qquad \mathcal{P}_{N-1} \mathcal{R}_N = \mathcal{L}_{N-1},$$

where $\mathcal{L}_{N-1} \colon Y \to Y_{N-1}$ is the Lagrange interpolation operator relevant to Θ_N.

Then, we observe that $\mathcal{M}_N$ is invertible if and only if, for every $\Xi \in \mathbb{C}^{dN}$, there exists a unique $\Psi \in \mathbb{C}^{dN}$ such that

$$\mathcal{M}_N \Psi = \Xi. \tag{3.1}$$

In this case, let $\psi_N := \mathcal{P}_{0,N}\Psi$. From $\psi_N = \mathcal{V}_0 \psi_N'$, (2.7) and (3.1), we get

$$\mathcal{R}_N \mathcal{M} \mathcal{P}_{0,N} \Psi = \mathcal{R}_N (\mathcal{I}_Y - \mathcal{W}) \psi_N' = \Xi,$$

and by applying $\mathcal{P}_{N-1}$, since $\psi_N' = \mathcal{L}_{N-1}\psi_N'$, we obtain

$$(\mathcal{I}_Y - \mathcal{L}_{N-1}\mathcal{W})\psi_N' = \mathcal{P}_{N-1}\Xi. \tag{3.2}$$

Now, we prove that $\mathcal{M}_N$ is invertible by showing that (3.2) has a unique polynomial solution ψ_N' in X.

Lemma 3.1. *Under Assumption 3, we have that*

$$\|(\mathcal{I}_X - \mathcal{L}_{N-1}\mathcal{W}) - (\mathcal{I}_X - \mathcal{W})\|_{X \leftarrow X} \to 0, \qquad N \to \infty. \tag{3.3}$$

Moreover, there exists a positive integer $\bar{N}$ such that, for every integer $N \geq \bar{N}$, $\mathcal{I}_X - \mathcal{L}_{N-1}\mathcal{W}$ is invertible and

$$\left\|(\mathcal{I}_X - \mathcal{L}_{N-1}\mathcal{W})^{-1}\right\|_{X \leftarrow X} \leq 2 \left\|(\mathcal{I}_X - \mathcal{W})^{-1}\right\|_{X \leftarrow X}. \tag{3.4}$$

Finally, $\mathcal{M}_N\colon \mathbb{C}^{dN} \to \mathbb{C}^{dN}$ *is invertible for every integer* $N \geq \bar{N}$ *with inverse*

$$\mathcal{M}_N^{-1} \coloneqq \mathcal{R}_N \mathcal{V}_0 \left(\mathcal{I}_X - \mathcal{L}_{N-1}\mathcal{W}\right)^{-1} \mathcal{P}_{N-1}. \tag{3.5}$$

Proof. We use a proof technique similar to [10, Chapter 5]. Let us observe that

$$\mathcal{I}_X - \mathcal{L}_{N-1}\mathcal{W} = (\mathcal{I}_X - \mathcal{W}) + (\mathcal{I}_X - \mathcal{L}_{N-1})\,\mathcal{W}.$$

Now, since $\mathrm{Range}(\mathcal{W}) \subset Y$ and $\mathcal{W}\colon X \to Y$ is bounded, Assumption 3 guarantees that there exists a positive constant C independent of N such that [35, Theorem 1]

$$\|\,(\mathcal{I}_X - \mathcal{L}_{N-1})\,\mathcal{W}\|_{X\leftarrow X} \leq C \cdot \|\mathcal{W}\|_{Y\leftarrow X} \cdot \frac{\log N}{N} \to 0, \qquad N \to \infty. \tag{3.6}$$

This gives (3.3). Then, the Banach perturbation Lemma [29, p. 142, Theorem 10.1] ensures that there exists $\bar{N} \in \mathbb{N}$ such that $\mathcal{I}_X - \mathcal{L}_{N-1}\mathcal{W}$ is invertible in X and (3.4) holds for every integer $N \geq \bar{N}$. Finally, (3.5) follows from (3.1) and (3.2). □

Note that, if $\Xi = \mathcal{R}_N\xi$, for $\xi \in Y$, then the unique polynomial solution ψ'_N of (3.2) is given by $\psi'_N = (\mathcal{I}_X - \mathcal{L}_{N-1}\mathcal{W})^{-1}\mathcal{J}\mathcal{L}_{N-1}\xi$. Hence, by introducing the operator $\widehat{\mathcal{M}}_N^{-1}\colon Y \to Y_{0,N}$ defined as

$$\widehat{\mathcal{M}}_N^{-1} \coloneqq \mathcal{V}_0(\mathcal{I}_X - \mathcal{L}_{N-1}\mathcal{W})^{-1}\mathcal{J}\mathcal{L}_{N-1}, \tag{3.7}$$

we have $\psi_N = \widehat{\mathcal{M}}_N^{-1}\xi$, and the following diagram commutes.

$$\begin{tikzcd}
Y \arrow[r, "\widehat{\mathcal{M}}_N^{-1}"] \arrow[d, "\mathcal{J}\mathcal{L}_{N-1}"'] & Y_0 \\
X \arrow[r, "(\mathcal{I}_X - \mathcal{L}_{N-1}\mathcal{W})^{-1}"'] & X \arrow[u, "\mathcal{V}_0"']
\end{tikzcd}$$

4. Convergence analysis. In this section, we investigate the convergence of the eigenvalues (and the corresponding eigenvectors) of $\mathcal{H}_N$ to those of $\mathcal{H}$ via the spectral approximation theory of [12]. To this aim, let us define the operator

$$\widehat{\mathcal{H}}_N \coloneqq \mathcal{P}_{N-1}\mathcal{H}_N\mathcal{R}_N\colon Y \to Y,$$

which has the same nonzero eigenvalues with the same geometric and partial multiplicities of $\mathcal{H}_N$ [9, Proposition 4.1]. Then, since $\widehat{\mathcal{H}}_N - \mathcal{H}$ is compact for every $N \geq \bar{N}$ thanks to Corollary 2.2, it is sufficient to show that [12, p. 498]

$$\|\widehat{\mathcal{H}}_N - \mathcal{H}\|_{Y\leftarrow Y} \to 0, \qquad N \to \infty. \tag{4.1}$$

From (3.7), we have that $\mathcal{L}_{0,N}\widehat{\mathcal{M}}_N^{-1} = \widehat{\mathcal{M}}_N^{-1}$, hence we can write

$$\widehat{\mathcal{H}}_N = \mathcal{L}_{N-1}\mathcal{B}\widehat{\mathcal{M}}_N^{-1},$$

and

$$\widehat{\mathcal{H}}_N - \mathcal{H} = (\mathcal{L}_{N-1} - \mathcal{I}_Y)\mathcal{B}(\widehat{\mathcal{M}}_N^{-1} - \mathcal{M}^{-1}) + (\mathcal{L}_{N-1} - \mathcal{I}_Y)\mathcal{B}\mathcal{M}^{-1} + \mathcal{B}(\widehat{\mathcal{M}}_N^{-1} - \mathcal{M}^{-1}).$$

Thus, in order to prove the convergence of $\widehat{\mathcal{H}}_N$ to $\mathcal{H}$, we need to investigate the behavior of $(\mathcal{L}_{N-1} - \mathcal{I}_Y)\mathcal{B}$ and $\widehat{\mathcal{M}}_N^{-1} - \mathcal{M}^{-1}$ as $N \to \infty$.

4.1. Convergence in norm of $\widehat{\mathcal{H}}_N$ to $\mathcal{H}$.

LEMMA 4.1. *Let Assumption* 3 *hold. Then*

$$\|\widehat{\mathcal{M}}_N^{-1}-\mathcal{M}^{-1}\|_{Y_0\leftarrow Y}\to 0, \qquad N\to\infty.$$

Proof. Observe that, from (2.8) and (3.7), we can write $\widehat{\mathcal{M}}_N^{-1}-\mathcal{M}^{-1}$ as

$$\widehat{\mathcal{M}}_N^{-1}-\mathcal{M}^{-1}=\mathcal{V}_0[(\mathcal{I}_X-\mathcal{L}_{N-1}\mathcal{W})^{-1}\mathcal{J}(\mathcal{L}_{N-1}-\mathcal{I}_Y)] \tag{4.2}$$

$$+\mathcal{V}_0[\big((\mathcal{I}_X-\mathcal{L}_{N-1}\mathcal{W})^{-1}-(\mathcal{I}_X-\mathcal{W})^{-1}\big)\mathcal{J}]. \tag{4.3}$$

Simple computations show that

$$(\mathcal{I}_X-\mathcal{L}_{N-1}\mathcal{W})^{-1}-(\mathcal{I}_X-\mathcal{W})^{-1}=(\mathcal{I}_X-\mathcal{L}_{N-1}\mathcal{W})^{-1}(\mathcal{L}_{N-1}-\mathcal{I}_X)\mathcal{W}(\mathcal{I}_X-\mathcal{W})^{-1}. \tag{4.4}$$

Hence, from (2.10) and (3.4), we get

$$\|\widehat{\mathcal{M}}_N^{-1}-\mathcal{M}^{-1}\|_{Y_0\leftarrow Y}\le C_1\,\|\mathcal{J}(\mathcal{L}_{N-1}-\mathcal{I}_Y)\|_{X\leftarrow Y} \tag{4.5}$$

$$+\frac{a^\dagger C_1^2}{2}\|(\mathcal{L}_{N-1}-\mathcal{I}_X)\mathcal{W}\|_{X\leftarrow X}, \tag{4.6}$$

where $C_1\coloneqq 2\|(\mathcal{I}_X-\mathcal{W})^{-1}\|_{X\leftarrow X}$. The term in (4.6) tends to zero as $N\to\infty$ thanks to (3.6). As for the term on the right-hand side of (4.5), Assumption 3 ensures that there exists a positive constant C_2 independent of N such that [35, Theorem 1]

$$\|\mathcal{J}(\mathcal{L}_{N-1}-\mathcal{I}_Y)\|_{X\leftarrow Y}\le C_2\cdot\frac{\log N}{N}\to 0, \qquad N\to\infty.$$

This completes the proof. ∎

Now, in order to prove (4.1), we make the following assumption.

ASSUMPTION 4. $\beta^+(\cdot,\alpha)\in C([0,a^\dagger],\mathbb{R}^{d\times d})$ *for almost all* $\alpha\in[0,a^\dagger]$.

THEOREM 4.2. *Let Assumption* 3 *and Assumption* 4 *hold. Then*

$$\|\widehat{\mathcal{H}}_N-\mathcal{H}\|_{Y\leftarrow Y}\to 0, \qquad N\to\infty.$$

Proof. Let us observe that

$$\|\widehat{\mathcal{H}}_N-\mathcal{H}\|_{Y\leftarrow Y}\le\|(\mathcal{L}_{N-1}-\mathcal{I}_Y)\mathcal{B}\|_{Y\leftarrow Y_0}\cdot\|\widehat{\mathcal{M}}_N^{-1}-\mathcal{M}^{-1}\|_{Y_0\leftarrow Y} \tag{4.7}$$

$$+\|(\mathcal{L}_{N-1}-\mathcal{I}_Y)\mathcal{B}\mathcal{M}^{-1}\|_{Y\leftarrow Y} \tag{4.8}$$

$$+\|\mathcal{B}\|_{Y\leftarrow Y_0}\cdot\|\widehat{\mathcal{M}}_N^{-1}-\mathcal{M}^{-1}\|_{Y_0\leftarrow Y}. \tag{4.9}$$

The term in (4.9) tends to zero as $N\to\infty$ thanks to Lemma 4.1. As for (4.7) and (4.8), let us recall that for every $\psi\in Y_0$ we have

$$\|(\mathcal{L}_{N-1}-\mathcal{I}_Y)\mathcal{B}\psi\|_Y=\left|(\mathcal{L}_{N-1}-\mathcal{I}_Y)\mathcal{B}\psi_{|a=0}\right|_{\mathbb{C}^d}+\left\|\left((\mathcal{L}_{N-1}-\mathcal{I}_Y)\mathcal{B}\psi\right)'\right\|_X. \tag{4.10}$$

The first term on the right-hand side of (4.10) tends to zero as $N\to\infty$ since $\mathcal{B}Y_0\subseteq Y$ ensures the convergence of the Lagrange interpolation at the Chebyshev zeros in the infinite-norm [30, Theorem 1]. As for the second term, Assumption 4 guarantees that $(\mathcal{B}\psi)'\in C([0,a^\dagger],\mathbb{C}^d)$. Thus, by applying [39, Theorem 1 and Corollary], which establish the convergence of the derivative of Lagrange interpolation at the Chebyshev zeros in the X-norm, we get

$$\|(\mathcal{L}_{N-1}\mathcal{B}\psi)' - (\mathcal{B}\psi)'\|_X \to 0, \qquad N \to \infty.$$

[29, Theorem 10.6] states that if $\{\mathcal{A}_N\}_{N\in\mathbb{N}}$ is a pointwise convergent sequence of bounded linear operators $\mathcal{A}_N\colon Y_0 \to Y$ with limit operator $\mathcal{A}\colon Y_0 \to Y$, and $\mathcal{K}\colon Y \to Y_0$ is compact, then $\|(\mathcal{A}_N - \mathcal{A})\mathcal{K}\|_{Y\leftarrow Y} \to 0$ as $N \to \infty$. Applying this theorem with $\mathcal{A}_N = \mathcal{L}_{N-1}\mathcal{B}$, $\mathcal{A} = \mathcal{B}$ and $\mathcal{K} = \mathcal{M}^{-1}$, we conclude that (4.8) tends to zero as $N \to \infty$.

Finally, from the uniform boundedness principle [11, p. 32, Theorem 2.2], we get

$$\sup_{N\in\mathbb{N}} \|(\mathcal{L}_{N-1} - \mathcal{I}_Y)\mathcal{B}\|_{Y\leftarrow Y_0} < +\infty. \tag{4.11}$$

Hence, (4.7) tends to zero as $N \to \infty$ thanks to Lemma 4.1. ∎

4.2. Convergence of eigenvalues and eigenspaces.

THEOREM 4.3. *Let Assumption* 3 *and Assumption* 4 *hold. Let $\lambda \in \mathbb{C}$ be an isolated nonzero eigenvalue of $\mathcal{H}$ with finite algebraic multiplicity m and ascent l and let Δ be a neighborhood of λ such that λ is the sole eigenvalue of $\mathcal{H}$ in Δ. Then there exists $\bar{N}$ such that, for $N \geq \bar{N}$, $\widehat{\mathcal{H}}_N$ has in Δ exactly m eigenvalues $\lambda_{N,i}$, $i = 1, \ldots, m$, counting their multiplicities. Moreover,*

$$\max_{i=1,\ldots,m} |\lambda_{N,i} - \lambda| = O\big(\varepsilon_N^{1/l}\big)$$

where

$$\varepsilon_N \coloneqq \|\widehat{\mathcal{H}}_N - \mathcal{H}\|_{Y\leftarrow G_\lambda} \tag{4.12}$$

and G_λ is the generalized eigenspace of λ. Finally, for any $i = 1, \ldots, m$ and for any eigenfunction $\psi_{N,i}$ of $\widehat{\mathcal{H}}_N$ relevant to $\lambda_{N,i}$ such that $\|\psi_{N,i}\|_Y = 1$, we have

$$\operatorname{dist}(\psi_{N,i},\ \ker(\lambda\mathcal{I}_Y - \mathcal{H})) = O(\varepsilon_N^{1/l}),$$

where dist *is the distance in the space Y between an element and a subspace.*

Proof. The claim follows by applying [12, Proposition 2.3 and Proposition 4.1]. ∎

Now, we complete the analysis with error bounds under each of the following regularity conditions.

ASSUMPTION 5.

(i) $\beta^+, \beta^- \in W^{s,\infty}([0, a^\dagger]^2, \mathbb{R}^{d\times d})$ *and* $\delta \in W^{s,\infty}([0, a^\dagger], \mathbb{R}^{d\times d})$ *for some integer* $s \geq 1$*,*

(ii) $\beta^+, \beta^- \in C^\infty([0, a^\dagger]^2, \mathbb{R}^{d\times d})$ *and* $\delta \in C^\infty([0, a^\dagger], \mathbb{R}^{d\times d})$*,*

(iii) β^+, β^-, δ *are real analytic.*

COROLLARY 4.4. *Let λ, $\lambda_{N,i}$, $i = 1, \ldots, m$, ε_N, and G_λ be as in Theorem 4.3, and let Assumption* 3 *and Assumption* 5 *hold. Then $\varepsilon_N = O(\rho_N)$, where*

$$\rho_N \coloneqq \begin{cases} N^{-s}\log N & \text{under Assumption 5 } (i), \\ N^{-r}\log N & \text{for every integer } r \geq 1 \text{ under Assumption 5 } (ii), \\ p^{-N}\log N & \text{for some constant } p > 1 \text{ under Assumption 5 } (iii). \end{cases}$$

Proof. Since the generalized eigenspace G_λ has finite dimension m, it is enough to show that $\|(\widehat{\mathcal{H}}_N - \mathcal{H})\psi_{\lambda,i}\|_Y = O(\rho_N)$ for all $i = 1, \dots, m$, where $\{\psi_{\lambda,i}\}_{i=1}^m$ is a basis of G_λ. Then the claim will follow by proceeding as in the proof of [8, Proposition 4.9]. For $\psi_\lambda \in \{\psi_{\lambda,i}\}_{i=1}^m$, from (3.4), (4.2)-(4.4), (4.7)-(4.9) and (4.11), we have

$$
\begin{aligned}
&\|(\widehat{\mathcal{H}}_N - \mathcal{H})\psi_\lambda\|_Y \leq C\big(\|\mathcal{J}(\mathcal{L}_{N-1} - \mathcal{I}_Y)\psi_\lambda\|_X && (4.13)\\
&\qquad + \|(\mathcal{L}_{N-1} - \mathcal{I}_X)\mathcal{W}(\mathcal{I}_X - \mathcal{W})^{-1}\psi_\lambda\|_X\big) && (4.14)\\
&\qquad + \|(\mathcal{L}_{N-1} - \mathcal{I}_Y)\mathcal{H}\psi_\lambda\|_Y, && (4.15)
\end{aligned}
$$

where

$$C \coloneqq 2\|(\mathcal{I}_X - \mathcal{W})^{-1}\|_{X\leftarrow X}\left(\sup_{N\in\mathbb{N}} \|(\mathcal{L}_{N-1} - \mathcal{I}_Y)\mathcal{B}\|_{Y\leftarrow Y_0} + \|\mathcal{B}\|_{Y\leftarrow Y_0}\right).$$

Moreover, for $\mathcal{T} \in \{\mathcal{I}_Y, \mathcal{H}, \mathcal{W}(\mathcal{I}_X - \mathcal{W})^{-1}\mathcal{J}\}$, we have

(*i*) $\mathcal{T}(G_\lambda) \subset W^{s+1,\infty}([0, a^\dagger], \mathbb{C}^d)$ under Assumption 5 (*i*),

(*ii*) $\mathcal{T}(G_\lambda) \subset C^\infty([0, a^\dagger], \mathbb{C}^d)$ under Assumption 5 (*ii*),

(*iii*) $\mathcal{T}(G_\lambda)$ consists of real analytic functions under Assumption 5 (*iii*).

Hence, we can bound the term on the right-hand side of (4.13) as follows

$$\|\mathcal{J}(\mathcal{L}_{N-1} - \mathcal{I}_Y)\psi_\lambda\|_X \leq a^\dagger\|(\mathcal{L}_{N-1} - \mathcal{I}_Y)\psi_\lambda\|_\infty,$$

and, from Jackson's type theorems [37, Section 1.1.2], [43, Chapters 7 and 8] we get

$$\|(\mathcal{L}_{N-1} - \mathcal{I}_Y)\psi_\lambda\|_\infty \leq O\left((1 + \Lambda_{N-1})E_{N-1}(\psi_\lambda)\right) = O(\rho_N),$$

where Λ_{N-1} is the Lebesgue constant relevant to Θ_N, that under Assumption 3 is $O(\log N)$, and $E_{N-1}(\psi_\lambda)$ is the best uniform approximation error of ψ_λ in the space of polynomials of degree at most $N-1$. The term in (4.14) can be bounded as

$$\|(\mathcal{L}_{N-1} - \mathcal{I}_X)\mathcal{W}(\mathcal{I}_X - \mathcal{W})^{-1}\psi_\lambda\|_X \leq\ a^\dagger\|(\mathcal{L}_{N-1} - \mathcal{I}_Y)\mathcal{W}(\mathcal{I}_X - \mathcal{W})^{-1}\psi_\lambda\|_\infty,$$

which, in turn, can be bounded as

$$
\begin{aligned}
\|(\mathcal{L}_{N-1} - \mathcal{I}_Y)\mathcal{W}(\mathcal{I}_X - \mathcal{W})^{-1}\psi_\lambda\|_\infty &\leq O\left((1 + \Lambda_{N-1})E_{N-1}(\mathcal{W}(\mathcal{I}_X - \mathcal{W})^{-1}\psi_\lambda)\right)\\
&= O(\rho_N).
\end{aligned}
$$

Finally, the term in (4.15) can be bounded as

$$\|(\mathcal{L}_{N-1} - \mathcal{I}_Y)\mathcal{H}\psi_\lambda\|_Y \leq\ \|(\mathcal{L}_{N-1} - \mathcal{I}_Y)\mathcal{H}\psi_\lambda\|_\infty + a^\dagger\left\|((\mathcal{L}_{N-1} - \mathcal{I}_Y)\mathcal{H}\psi_\lambda)'\right\|_\infty.$$

For these, from [37, Section 1.1.2] and [43, Chapters 7 and 8] we get

$$\|(\mathcal{L}_{N-1} - \mathcal{I}_Y)\mathcal{H}\psi_\lambda\|_\infty = O\left((1 + \Lambda_{N-1})E_{N-1}(\mathcal{H}\psi_\lambda)\right) = O(\rho_N),$$

and, from [34, p. 269, Theorem 4.2.11] we get

$$\|((\mathcal{L}_{N-1} - \mathcal{I}_Y)\mathcal{H}\psi_\lambda)'\|_\infty = O\left((1 + \Lambda_{N-1})E_{N-2}\left((\mathcal{H}\psi_\lambda)'\right)\right) = O(\rho_N). \qquad \square$$

Remark 4.5. One can show that, under Assumption 5 (*i*), the convergence of $R_N = \rho(\mathcal{H}_N)$ to the true reproduction number R gains one order compared to ρ_N, i.e., it has order $O((N^{-(s+1)}\log N)^{1/l})$. In fact, using the birth operator $\mathcal{B}$ and the transition operator $\mathcal{M}$, we can consider the compact operator $\mathcal{M}^{-1}\mathcal{B} : Y \to D(\mathcal{M})$, whose nonzero eigenvalues λ coincide with those of $\mathcal{H}$ and have the same algebraic multiplicities and ascents. The eigenfunctions φ_λ of $\mathcal{M}^{-1}\mathcal{B}$ (corresponding to λ) belong to $D(\mathcal{M})$ and satisfy $\varphi_\lambda = \mathcal{M}^{-1}\psi_\lambda$, where ψ_λ are the corresponding eigenfunctions of $\mathcal{H}$. The reproduction number R is also the spectral radius of $\mathcal{M}^{-1}\mathcal{B}$, providing an alternative way to approximate it through the spectral radius of the matrix $\mathcal{M}_N^{-1}\mathcal{B}_N$. It is easy to see that the matrices $\mathcal{M}_N^{-1}\mathcal{B}_N$ and $\mathcal{B}_N\mathcal{M}_N^{-1}$ are similar, hence they have the same eigenvalues for every $N \geq 1$. The convergence analysis can be carried out as before. The operator $\mathcal{P}_{N,0}\mathcal{M}_N^{-1}\mathcal{B}_N\mathcal{R}_N : Y \to Y_{0,N}$ has the same nonzero eigenvalues with the same geometric and partial multiplicities of $\mathcal{M}_N^{-1}\mathcal{B}_N$ [9, Proposition 4.1], and from (3.7) it can be expressed as $\widehat{\mathcal{M}}_N^{-1}\mathcal{B}\mathcal{L}_{N,0}$. Moreover, since $\mathrm{Range}(\widehat{\mathcal{M}}_N^{-1}) \subset Y_{0,N}$, $\widehat{\mathcal{M}}_N^{-1}\mathcal{B}\mathcal{L}_{N,0}$ has the same nonzero eigenvalues with the same geometric and partial multiplicities, and the same eigenfunctions as the operator $\widehat{\mathcal{M}}_N^{-1}\mathcal{B}$ [9, Proposition 4.3]. The norm convergence of $\widehat{\mathcal{M}}_N^{-1}\mathcal{B}$ to $\mathcal{M}^{-1}\mathcal{B}$ easily follows from Lemma 4.1, and an analogous of Theorem 4.3 can be derived. The main difference is that, since the convergence order of the approximation error of the eigenvalue λ is driven by the interpolation error of $\mathcal{M}^{-1}\mathcal{B}\varphi_\lambda$, which under Assumption 5 (i) has one more degree of smoothness compared to $\mathcal{H}\psi_\lambda$, we get that $|R - R_N| = O((N^{-(s+1)}\log N)^{1/l})$. Example 1 in section 6 illustrates this behavior.

5. Implementation issues. Here we give an explicit description of the entries of the matrices $\mathcal{B}_N$ and $\mathcal{M}_N$. For the sake of simplicity, we restrict to the case $d = 1$.

Thanks to the cardinal property of the Lagrange polynomials ($\ell_{0,j}(a_i) = \delta_{ij}$, $i, j = 0, \dots, N$, where δ_{ij} is Kronecker's Delta), it is easy to see that the entries of the matrices are explicitly given by

$$(\mathcal{B}_N)_{ij} = \int_0^{a_i}\int_0^{a^\dagger} \beta^+(\zeta,\alpha)\ell'_{0,j}(\alpha)\,\mathrm{d}\alpha\,\mathrm{d}\zeta + \int_0^{a^\dagger} b^+(\alpha)\ell'_{0,j}(\alpha)\,\mathrm{d}\alpha, \qquad i, j = 1, \dots N, \tag{5.1}$$

and

$$\begin{aligned}(\mathcal{M}_N)_{ij} = \ell'_{0,j}(a_i) &- \int_0^{a_i} \delta(\alpha)\ell'_{0,j}(\alpha)\,\mathrm{d}\alpha \\ &- \int_0^{a_i}\int_0^{a^\dagger} \beta^-(\zeta,\alpha)\ell'_{0,j}(\alpha)\,\mathrm{d}\alpha\,\mathrm{d}\zeta \\ &+ \int_0^{a^\dagger} b^-(\alpha)\ell'_{0,j}(\alpha)\,\mathrm{d}\alpha, \qquad i, j = 1, \dots N.\end{aligned} \tag{5.2}$$

When the integrals in (5.1) and (5.2) cannot be computed analytically, we approximate them via a quadrature formula. For the integrals in $[0, a^\dagger]$, we use the Fejer's first rule quadrature formula [48], and for the integrals in $[0, a_i]$, $i = 1, \dots, N$, we use the quadrature weights given by the i-th row of the inverse of the differentiation matrix [18]

$$(\mathcal{D}_N)_{ij} \coloneqq \ell'_{0,j}(a_i), \quad i, j = 1, \dots, N.$$

In this case, the bounds in Corollary 4.4 are preserved under the following regularity conditions (see [14, p. 85] and [42]).

Assumption 6.
(i) $b^+, b^- \in W^{s,\infty}([0, a^\dagger], \mathbb{R}^{d\times d})$ *for some integer* $s \geq 1$,
(ii) $b^+, b^- \in C^\infty([0, a^\dagger], \mathbb{R}^{d\times d})$,
(iii) b^+, b^- *are real analytic.*

In the presence of discontinuities in the model coefficients or in their derivatives, a piecewise approach can be used. In this case, one may choose as discretization points either the Chebyshev zeros extended with the left endpoint, or, to simplify the implementation, the Chebyshev extremal nodes [34, 42, 43]. In the latter case, to approximate the integrals in $[0, a^\dagger]$ we use the Clenshaw–Curtis quadrature formula [13]. Note that the MATLAB demos available at http://cdlab.uniud.it/software used to make all the tests in section 6 implement these piecewise alternatives.

6. Numerical results. In this section, we apply the numerical method to some instances of (2.1) to experimentally validate the theoretical results in section 4. In particular, we aim to illustrate the link between the convergence order of the numerical approximation R_N of R and the approximation error of the relevant eigenspaces (see Theorem 4.3 and Remark 4.5). The latter depends on the regularity of the (generalized) eigenfunctions through the smoothness of the model parameters, see Corollary 4.4 and Remark 4.5. Thus, the first two examples are constructed to have explicit expressions for R and the associated eigenfunctions. Both examples are scalar and represent the linearized equation for the infected individuals around the disease-free equilibrium. The first example is structured by demographic age (without vertical transmission), whereas the second one is structured by infection age, where the infection process is described by a boundary condition, to analyze the effect of the quadrature error. As final example we propose a three-dimensional model structured by demographic age, with horizontal and vertical transmission, and with piecewise C^∞ coefficients estimated from real data. In this case, analytic expressions for R and the relevant eigenfunctions are not available. Hence, the errors are computed with respect to reference values (obtained with $N = 120$). In all these examples, we compare the approximation errors of R by using either the N Chebyshev zeros extended with the left endpoint or the $N + 1$ Chebyshev extrema.

Example 1. Motivated by the Susceptible-Infected-Removed (SIR) model structured by demographic age without vertical transmission (see [24, Chapter VI] and [27, Chapter 6]), we consider the model (2.1) with $d = 1$, and parameters

$$\beta(a, \alpha) = \frac{1}{c} q(a)(a^\dagger - \alpha), \qquad b(a) \equiv 0, \qquad \delta(a) \equiv -\gamma,$$

where $a^\dagger, \gamma > 0$, q is a given nonnegative function and, for any choice of q,

$$c := \int_0^{a^\dagger} (a^\dagger - a) \int_0^a e^{-\gamma(a-\alpha)} q(\alpha)\, \mathrm{d}\alpha\, \mathrm{d}a.$$

With this choice of parameters, the basic reproduction number is exactly $R_0 = 1$, and is obtained in our framework by taking $\beta^+ = \beta$, $\beta^- \equiv 0$ and $b^+ = b^- \equiv 0$. $\mathcal{H}$ is a rank-one operator and the eigenfunction relevant to $R = R_0$ is explicitly known: $\psi(a) = \int_0^a q(s)\, \mathrm{d}s$, $a \in [0, a^\dagger]$. Moreover, with reference to Remark 4.5, $\varphi(a) = (\mathcal{M}^{-1}\psi)(a) = \int_0^a e^{-\gamma(a-\alpha)}\psi(\alpha)\, \mathrm{d}\alpha$, $a \in [0, a^\dagger]$.

Figure 1 and Figure 2 show, for increasing N, the errors $|R - R_N|$ and $|(\mathcal{H} - \widehat{\mathcal{H}}_N)\psi_{|a=0}|_{\mathbb{C}^d} + \|((\mathcal{H} - \widehat{\mathcal{H}}_N)\psi)'\|_\infty$, which gives a bound to ε_N in (4.12), with $a^\dagger = \gamma = 1$, and for three different choices of q, namely $q(a) = e^{-2a}$ (analytic, Figure 1, left),

$q(a) = e^{-(x-0.5)^{-2}}(x-0.5)^{-2}\chi_{[0.5,a^\dagger]}(a)$ (C^∞, Figure 1, right) and $q(a) = (0.5-a)^2|0.5-a|$ ($W^{3,\infty}$, Figure 2). The infinite norm is estimated by computing the maximum absolute value over a mesh of 10^4 equidistant points in $[0, a^\dagger]$.

In Figure 1, we observe infinite convergence order, being the relevant eigenfunction ψ either analytic or C^∞, confirming the validity of Corollary 4.4 under Assumption 5 (*ii*) and (*iii*), respectively. Figure 2 shows order 4 for the approximation error of R (left and right), order 3 for $|(\mathcal{H}-\widehat{\mathcal{H}}_N)\psi_{|a=0}|_{\mathbb{C}^d} + \|((\mathcal{H}-\widehat{\mathcal{H}}_N)\psi)'\|_\infty$ (left), and order 4 for the error $\|((\mathcal{M}-\widehat{\mathcal{M}}_N^{-1})\mathcal{B}\varphi)'\|_\infty$ (right), in accordance with Remark 4.5. Note that, in all the three cases, the behavior of the approximation error for the Chebyshev extrema is similar to that of the Chebyshev zeros extended with the left endpoint.

Figure 3 illustrates how the behavior of the approximation error of R depends on the magnitude of the recovery rate γ and on the length of the age interval $a^\dagger$. In particular, we observe that, in the case of large values of γ or $a^\dagger$, a larger number of points N is required to obtain small approximation errors. This can be explained from the fact that the approximation error is related to the interpolation error on the exponential function $e^{-\gamma a}$ in the operator $\mathcal{M}^{-1}$, which depends on the derivative of the function (whose norm increases with γ) and on the length of the interval. For large age intervals, the approximation error can be reduced by resorting to a piecewise approach, splitting the age-interval in smaller regions. As an example, in Figure 4 we illustrate the results obtained with the piecewise version of the method for the case $a^\dagger = 30$ and $\gamma = 100$. Therein, we split the age interval in 6 sub-intervals, and we use a polynomial of degree N in each of them. Note the different behavior between the case of odd and even Chebyshev zeros.

Remark 6.1. In real-world applications, both $a^\dagger$ and γ may be large. For instance: in a model for human populations structured by demographic age, $a^\dagger$ is typically assumed to be equal or larger than 75 (yr), while in epidemiology γ could be assumed to be larger than 30 (yr^{-1}) for diseases that last less than 10 days on average. See for instance [1] or Example 3.

Example 2. We consider an SIR model where infected individuals are structured by infection age, see for example [24, Chapter 7]. The linearized equation for the infected individuals around the disease-free equilibrium can be recast as (2.1) by taking $d = 1$, $\beta(a,\alpha) \equiv 0$ and $\delta(a) \equiv -\gamma$, for $\gamma > 0$. In the following, we do not consider the presence of control measures.

To investigate the convergence of our method, we consider the following explicit expression for the basic reproduction number R_0 [27, Section 5.3]:

$$R_0 = \int_0^{a^\dagger} \beta(a) e^{-\int_0^a \gamma(\alpha)\,\mathrm{d}\alpha}\,\mathrm{d}a. \tag{6.1}$$

We take $a^\dagger = 14$, and b and γ such that $b(a)e^{-\gamma a} = \Gamma(k,\theta)(a)$, where $\Gamma(k,\theta)$ is a truncated Gamma density function with shape parameter $k > 0$ and scale parameter $\theta > 0$, normalized in the interval $[0, a^\dagger]$ [15, Section 4.1]. In particular we take $b(a) = ca^k$, $\gamma = 1/\theta$, and $\theta = 0.25$, where $c := \|\Gamma(k,\theta)\|_X^{-1}$. For this choice, from (6.1), we get that $R_0 = 1$. In our framework, we take $b^+ = b$ and $b^- \equiv 0$. The relevant eigenfunction is constant.

Figure 5 shows the behavior of the approximation error of $R = R_0$ for $k = 2$ and $k = \pi$, see [38, Table 1]. The method converges with infinite order for $k = 2$, i.e., when b is of class C^∞. Finite convergence order is observed for $k = \pi$, i.e., when b'' has a pole in $a = 0$. This illustrates how the quadrature errors affect the convergence

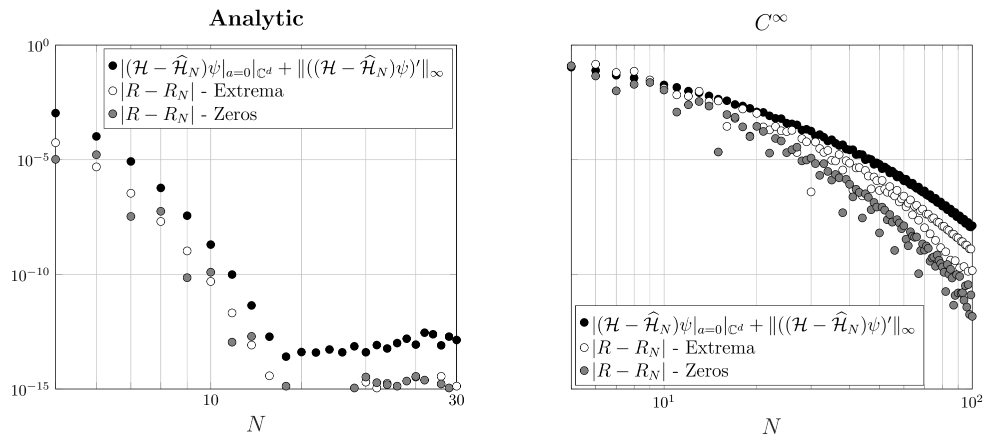

FIG. 1. *Example 1 with $q(a) = e^{-2a}$ (analytic, left) and $q(a) = e^{-(x-0.5)^{-2}}(x-0.5)^{-2}\chi_{[0.5,a^\dagger]}(a)$ (C^∞, right), with $a^\dagger = \gamma = 1$. Log-log plot for increasing N of the approximation error of R (white dots for the $N+1$ Chebyshev extrema and gray dots for the N Chebyshev zeros extended with the left endpoint) and the error $|(\mathcal{H}-\widehat{\mathcal{H}}_N)\psi_{|a=0}|_{\mathbb{C}^d}+\|((\mathcal{H}-\widehat{\mathcal{H}}_N)\psi)'\|_\infty$ for the discretization at the Chebyshev zeros extended with the left endpoint (black dots). Infinite order of convergence is observed in both panels, in agreement with Corollary* 4.4.

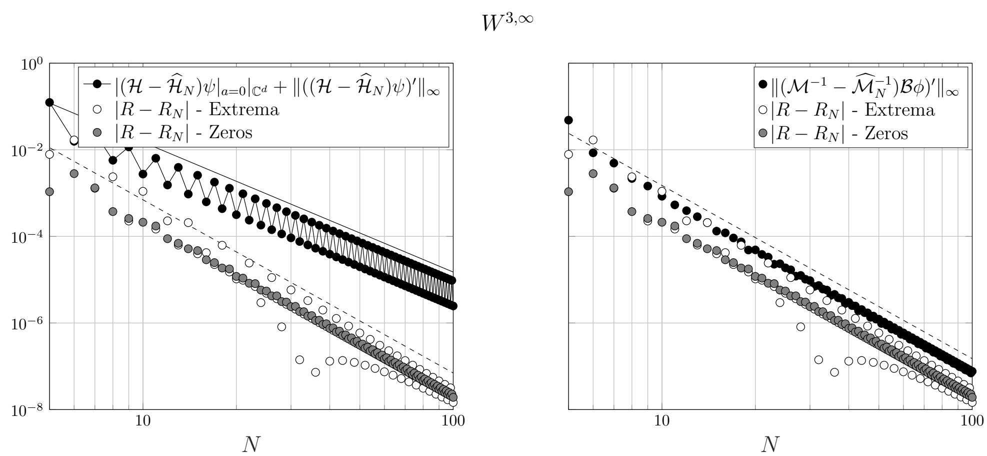

FIG. 2. *Example 1 with $q(a) = (0.5-a)^2|0.5-a|$ ($W^{3,\infty}$) and $a^\dagger = \gamma = 1$. Left panel: log-log plot for increasing N of the approximation error of R (white dots for the $N+1$ Chebyshev extrema and gray dots for the N Chebyshev zeros extended with the left endpoint) computed as $\rho(\mathcal{H}_N)$, and the error $|(\mathcal{H}-\widehat{\mathcal{H}}_N)\psi_{|a=0}|_{\mathbb{C}^d}+\|((\mathcal{H}-\widehat{\mathcal{H}}_N)\psi)'\|_\infty$ for the discretization at the Chebyshev zeros extended with the left endpoint (black dots). Convergence of order* 4 *and order* 3 *is observed for $|R-R_N|$ and $|(\mathcal{H}-\widehat{\mathcal{H}}_N)\psi_{|a=0}|_{\mathbb{C}^d}+\|((\mathcal{H}-\widehat{\mathcal{H}}_N)\psi)'\|_\infty$, respectively. Right panel: log-log plot for increasing N of the approximation error of R (white dots for the $N+1$ Chebyshev extrema and gray dots for the N Chebyshev zeros extended with the left endpoint) computed as $\rho(\mathcal{M}_N^{-1}\mathcal{B}_N)$, and the error $\|((\mathcal{M}-\widehat{\mathcal{M}}_N^{-1})\mathcal{B}\phi)'\|_\infty$ for the discretization at the Chebyshev zeros extended with the left endpoint. Convergence of order* 4 *is observed for all the errors, in agreement with Remark* 4.5*. The dashed lines have slope -4, while the solid line has slope -3.*

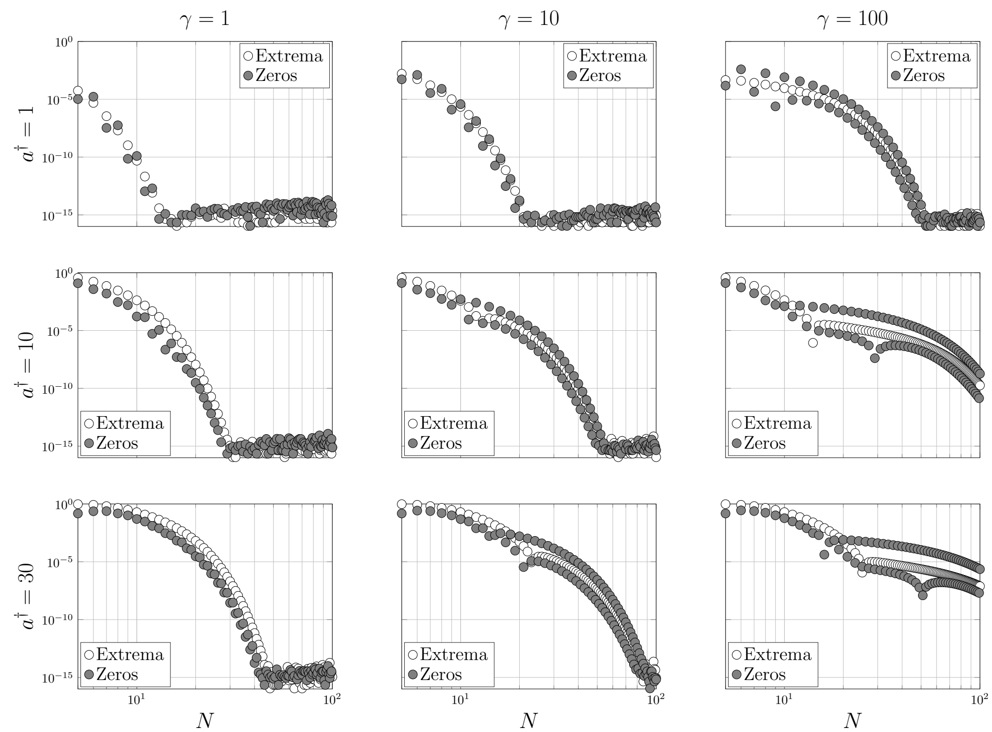

FIG. 3. *Example 1 with $q(a) = e^{-2a}$. Log-log plot for increasing N of the approximation error of R (white dots for the $N+1$ Chebyshev extrema and gray dots for the N Chebyshev zeros extended with the left endpoint) varying $a^\dagger$ and γ.*

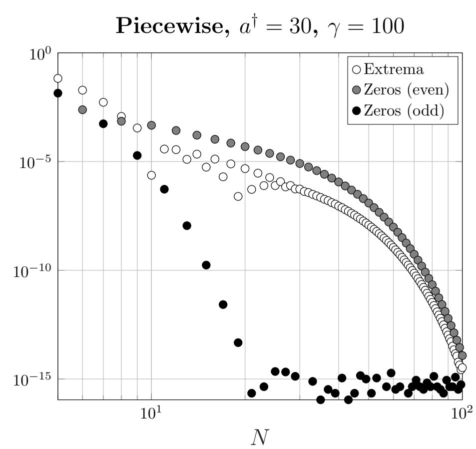

FIG. 4. *Example 1 with $q(a) = e^{-2a}$, $a^\dagger = 30$ and $\gamma = 100$. Log-log plot for increasing N of the piecewise approximation error of R (white dots for the $N+1$ Chebyshev extrema, gray and black dots for the N Chebyshev zeros extended with the left endpoint with N even and N odd, respectively). Note the different behavior of the error for odd and even N for the Chebyshev zeros.*

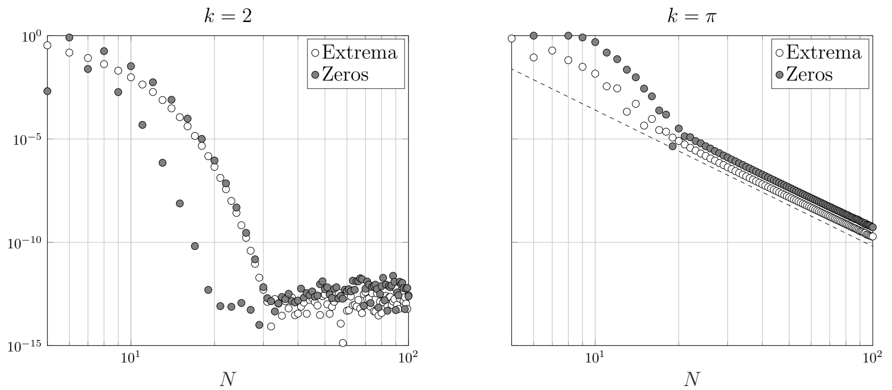

FIG. 5. *Example 2. Log-log plot of the approximation error for increasing N of $R = 1$ (white dots for the $N + 1$ Chebyshev extrema and gray dots for the N Chebyshev zeros extended with the left endpoint), for $k = 2$ (left) and $k = \pi$ (right). The slope of the dashed line is -6.5.*

order on R, even in the case of a constant eigenfunction. As pointed out in [38], in this case the order of convergence can be improved by computing the integrals, for example, with the MATLAB built-in integral function.

Example 3. We consider a model inspired by [49, 50] for the spread of Hepatitis B (HBV) in China, and we refer to [33] for a recent review of other models of the literature. Let $S(t, a)$, $L(t, a)$, $I(t, a)$, $C(t, a)$, $R(t, a)$ and $V(t, a)$ denote the density of individuals that are susceptible, latent (infected but not infectious), acutely infected, chronically infected, recovered, and vaccinated, respectively, at time $t \geq 0$ and demographic age $a \in [0, a^\dagger]$. The model reads

$$\begin{cases} \mathcal{D}S(t,a) = \omega V(t,a) - (\mu(a) + \lambda(t,a) + \nu(a))S(t,a), \\ \mathcal{D}L(t,a) = \lambda(t,a)S(t,a) - (\mu(a) + \sigma)L(t,a), \\ \mathcal{D}I(t,a) = \sigma L(t,a) - (\mu(a) + \gamma_1)I(t,a), \\ \mathcal{D}C(t,a) = p(a)\gamma_1 I(t,a) - (\mu(a) + \gamma_2(a))C(t,a), \\ \mathcal{D}R(t,a) = \gamma_2(a)C(t,a) + (1 - p(a))\gamma_1 I(t,a) - \mu(a)R(t,a), \\ \mathcal{D}V(t,a) = \nu(a)S(t,a) - (\omega + \mu(a))V(t,a), \end{cases}$$

for $t \geq 0$ and $a \in [0, a^\dagger]$, with boundary conditions [19]

$$\begin{cases} S(t,0) = \theta \displaystyle\int_0^{a^\dagger} f(a)\left(P(t,a) - q_1 I(t,a) - q_2 C(t,a)\right) \mathrm{d}a, \\ L(t,0) = \theta \displaystyle\int_0^{a^\dagger} f(a)\left(q_1 I(t,a) + q_2 C(t,a)\right) \mathrm{d}a, \\ V(t,0) = (1-\theta) \displaystyle\int_0^{a^\dagger} f(a) P(t,a)\, \mathrm{d}a, \\ I(t,0) = C(t,0) = R(t,0) = 0, \end{cases}$$

for $t \geq 0$, where [19, 47]

$$\lambda(t,a) = \int_0^{a^\dagger} \hat{k}(a,\alpha) \frac{I(t,\alpha) + \epsilon C(t,\alpha)}{\int_0^{a^\dagger} P(t,a)\,\mathrm{d}a} \mathrm{d}\alpha,$$

and $P := S + L + I + R + V + C$. Here, μ is the natural mortality rate (yr^{-1}), f is the per capita birth rate (yr^{-1}), $\hat{k}$ is the per capita transmission rate (yr^{-1}), ϵ is the relative transmission rate of chronic carriers, σ is the rate of moving from latent to infectious phase (yr^{-1}), γ_1 is the rate of moving from acute infection to recovered or chronic (yr^{-1}), p is the probability of becoming chronic instead of recovering, γ_2 is the recovery rate of chronic infection (yr^{-1}), ν is the per capita vaccination rate of individuals of age $a > 0$ (yr^{-1}), ω is the rate of waning of vaccine-induced immunity (yr^{-1}), q_1 and q_2 are the fractions of perinatally infected from individuals in the acute and chronic phase, respectively, and θ is the fraction of failed vaccinations at birth. We assume that the host population is at a demographic steady state, i.e., $\int_0^{a^\dagger} f(a)\Pi(a)\,\mathrm{d}a = 1$ holds for $\Pi(a) := \exp(-\int_0^a \mu(\xi)\,\mathrm{d}\xi)$, and that it has already attained the stationary age density

$$P(t,a) \equiv P^*(a) = P_0\Pi(a) \left(\int_0^{a^\dagger} \Pi(\xi)\,\mathrm{d}\xi \right)^{-1}, \qquad a \in [0, a^\dagger],$$

for some $P_0 > 0$ [27, Chapter 8]. Then, by defining $s := S/P$, $l := L/P$, $i := I/P$, $c := C/P$, $r := R/P$, and $v := V/P$, the resulting model has the disease-free equilibrium $(s^*, l^*, i^*, c^*, r^*, v^*) = (s^*, 0, 0, 0, 0, 1 - s^*)$, where

$$s^*(a) = \theta \mathrm{e}^{-\omega a - \int_0^a \nu(\alpha)\,\mathrm{d}\alpha} + \omega \int_0^a \mathrm{e}^{-\omega(a-s) - \int_s^a \nu(\alpha)\,\mathrm{d}\alpha}\,\mathrm{d}s, \qquad a \in [0, a^\dagger].$$

Observe that, in the absence of vaccination ($\nu \equiv 0$ and $\theta = 1$), we have $s^* \equiv 1$. The linearized equations for the infected individuals around the disease-free equilibrium read

$$\text{(6.2)} \qquad \begin{cases} \mathcal{D}l(t,a) = s^*(a) \int_0^{a^\dagger} k(a,\alpha)(i(t,\alpha) + \epsilon c(t,\alpha))\,\mathrm{d}\alpha - \sigma l(t,a), \\ \mathcal{D}i(t,a) = \sigma l(t,a) - \gamma_1 i(t,a), \\ \mathcal{D}c(t,a) = p(a)\gamma_1 i(t,a) - \gamma_2(a)c(t,a), \\ l(t,0) = \theta \int_0^{a^\dagger} f(a)\Pi(a)\,(q_1 i(t,a) + q_2 c(t,a))\,\mathrm{d}a, \\ i(t,0) = 0, \\ c(t,0) = 0, \end{cases}$$

for $t \geq 0$, $a \in [0, a^\dagger]$, where $k(a,\alpha) := \hat{k}(a,\alpha)\Pi(a)(\int_0^{a^\dagger} \Pi(\xi)\,\mathrm{d}\xi)$. (6.2) can be recast as (2.1) by taking

$$\beta(a,\alpha) = s^*(a)k(a,\alpha) \begin{pmatrix} 0 & 1 & \epsilon \\ 0 & 0 & 0 \\ 0 & 0 & 0 \end{pmatrix}, \quad b(a) = \theta f(a)\Pi(a) \begin{pmatrix} 0 & q_1 & q_2 \\ 0 & 0 & 0 \\ 0 & 0 & 0 \end{pmatrix},$$

TABLE 1
Age-specific forces of infection λ_i's (yr^{-1}) derived from [49], and corresponding $\bar{k}_i$'s defining the entries of the WAIFW, for $i = 1, \ldots, 7$.

Age class (years)	$0-2$	$3-5$	$6-9$	$10-14$	$15-29$	$30-49$	$50-75$
λ_i (assumed)	0.112	0.079	0.049	0.024	0.006	0.013	0.008
$\bar{k}_i$ (computed)	1.070	0.607	0.338	0.149	0.027	0.068	0.041

and

$$\delta(a) = \begin{pmatrix} -\sigma & 0 & 0 \\ \sigma & -\gamma_1 & 0 \\ 0 & p(a)\gamma_1 & -\gamma_2 \end{pmatrix}.$$

For this model, we can compute three reproduction numbers: the basic reproduction number R_0, for $\beta^+ = \beta$, $\beta^- \equiv 0$, $b^+ = b$, $b^- \equiv 0$; the type reproduction number for horizontal transmission T_H, for $\beta^+ = \beta$, $\beta^- \equiv 0$, $b^+ \equiv 0$, $b^- = b$; and the type reproduction number for vertical transmission T_V, for $\beta^+ \equiv 0$, $\beta^- = \beta$, $b^+ = b$, $b^- \equiv 0$.

Following [19, 49, 50], we assume $a^\dagger = 75$, $\Pi \equiv 1$, $\epsilon = 0.16$, $\sigma = 6$, $\gamma_1 = 4$, $\gamma_2 = 0.025$, $\omega = 0.1$, $q_1 = 0.711$, $q_2 = 0.109$,

$$p(a) = 0.176501 \exp(-0.787711a) + 0.02116, \qquad a \in [0, a^\dagger],$$

$f(a) = 0.018\chi_{[18,a^\dagger]}(a)$ for $a \in [0, a^\dagger]$, and we vary ν, θ in $[0, 1]$. As for k, we estimate it from real data. In [49, Formula 2] the authors give the following form of the force of infection

$$\lambda(a) := \begin{cases} 0.13074116 - 1.362531 \cdot 10^{-2}a \\ \qquad\qquad + 4.6463 \cdot 10^{-4}a^2 - 4.89 \cdot 10^{-6}a^3, & a \in [0, 47.5], \\ \lambda(47.5), & a \in (47.5, a^\dagger], \end{cases} \tag{6.3}$$

which was estimated from serological data by applying the procedure described in [21]. Here, in order to estimate k, we assume that it is piecewise constant among different age-groups, i.e.,

$$k(a, \alpha) = k_{ij}, \quad \text{for} \quad (a, \alpha) \in [\bar{a}_{i-1}, \bar{a}_i) \times [\bar{a}_{j-1}, \bar{a}_j), \quad i, j = 1, \ldots, 7,$$

where the age groups are listed in Table 1. This gives us a *Who Acquires Infection From Whom* (WAIFW) matrix $(k_{ij})_{i,j=1,\ldots,7}$, which can be estimated by applying the procedure of [2, Appendix A].[1] For doing this, we need to assume a particular form for the WAIFW matrix (otherwise the estimation problem is over-determined). Here we chose the one described in [19, Table II] and we refer to [2, Appendix A] for other possible choices. More in detail, $(k_{ij})_{i,j=1,\ldots,7}$ is assumed to be symmetric with elements $k_{ij} = \bar{k}_i$ for $i \geq j$. Then, in order to simplify the estimation of k, we take the mean values among different age-intervals of the age-specific force of infection in (6.3), see Table 1. The age groups are chosen by merging the original age-group division considered in [49], so that the piecewise force of infection captures the main geometrical features of (6.3).

[1] We estimate k by using γ_1 as recovery parameter and by neglecting, in first approximation, the role of chronic carriers in the transmission pattern.

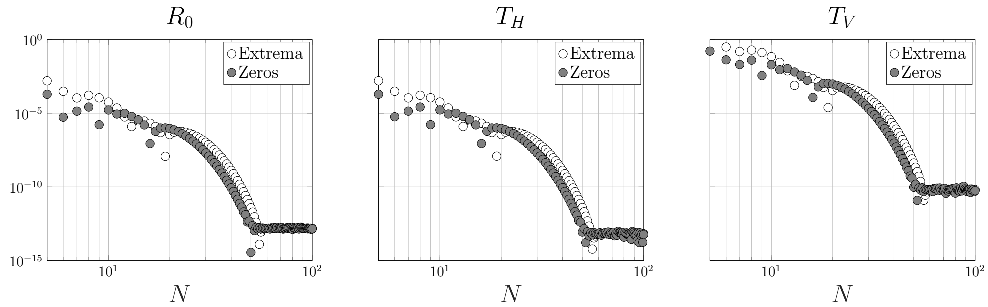

FIG. 6. *Example 3. Log-log plot of the absolute approximation errors for increasing N of R_0 (left), T_H (center) and T_V (right), with $\nu = 0.1$ and $\theta = 0.59$ (white dots for the $N + 1$ Chebyshev extrema and gray dots for the N Chebyshev zeros extended with the left endpoint). The reference values $R_0 \approx 1.048182936983250$, $T_H \approx 1.004493064088357$, and $T_V \approx 2.765546573797665$, are obtained with $N = 120$.*

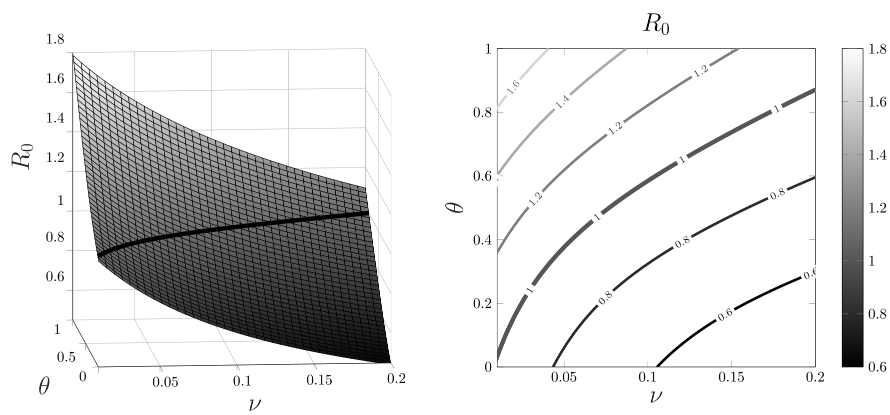

FIG. 7. *Example 3. R_0 as a function of ν and θ, with black line indicating $R_0 = 1$ (left) and relevant level curves (right) computed with $N = 50$.*

Figure 6 shows that the approximating reproduction numbers converge with infinite order, although $N \gtrsim 20$ nodes in each sub-interval are required to appreciate this behavior. This can be explained by the fact that, even though we are using a piecewise approach here, some of the age sub-intervals are large, as already discussed in Example 1.

Figure 7 shows a practical application of the method. Therein, the behavior of R_0 as a function of the fraction of failed vaccinations at birth θ and the per-capita vaccination rate ν is investigated. This shows that, even in the presence of vaccination, a large fraction of failed vaccinations at birth could lead to the spread of the epidemic, while this could be prevented for larger values of ν. Let us note that this result extends the one presented in [50, Figure 3], where the behavior of R_0 is investigated by neglecting the effect of vertical transmission.

Acknowledgments. This research was conducted while SDR was a PhD student at the Department of Mathematics, Computer Science and Physics of the University of Udine.

Conflict of interest. The authors declare there is no conflict of interest.

REFERENCES

[1] R. Anderson and B. Grenfell, *Quantitative investigations of different vaccination policies for the control of congenital rubella syndrome (CRS) in the United Kingdom*, Epidemiol. Infect., 96 (1986), pp. 305–333, https://doi.org/10.1017/s0022172400066079.

[2] R. Anderson and R. May, *Age-related changes in the rate of disease transmission: implications for the design of vaccination programmes*, Epidemiol. Infect., 94 (1985), pp. 365–436, https://doi.org/10.1017/S002217240006160X.

[3] C. Barril, À. Calsina, and J. Ripoll, *A practical approach to R_0 in continuous-time ecological models*, Math. Methods Appl. Sci., 41 (2018), pp. 8432–8445, https://doi.org/10.1002/mma.4673.

[4] J. P. Boyd, *Chebyshev and Fourier Spectral Methods*, Dover Publications, New York, 2nd ed., 2001.

[5] D. Breda, S. De Reggi, F. Scarabel, R. Vermiglio, and J. Wu, *Bivariate collocation for computing R_0 in epidemic models with two structures*, Comput. Math. with Appl., 116 (2022), pp. 15–24, https://doi.org/10.1016/j.camwa.2021.10.026.

[6] D. Breda, F. Florian, J. Ripoll, and R. Vermiglio, *Efficient numerical computation of the basic reproduction number for structured populations*, J. Comput. Appl. Math, 384 (2021), p. 113165, https://doi.org/10.1016/j.cam.2020.113165.

[7] D. Breda, T. Kuniya, J. Ripoll, and R. Vermiglio, *Collocation of next-generation operators for computing the basic reproduction number of structured populations*, J. Sci. Comput., 85 (2020), pp. 1–33, https://doi.org/10.1007/s10915-020-01339-1.

[8] D. Breda and D. Liessi, *Approximation of eigenvalues of evolution operators for linear renewal equations*, SIAM J. Numer. Anal., 56 (2018), pp. 1456–1481, https://doi.org/10.1137/17M1140534.

[9] D. Breda, S. Maset, and R. Vermiglio, *Approximation of eigenvalues of evolution operators for linear retarded functional differential equations*, SIAM J. Numer. Anal., 50 (2012), pp. 1456–1483, https://doi.org/10.1137/100815505.

[10] D. Breda, S. Maset, and R. Vermiglio, *Stability of Linear Delay Differential Equations: A Numerical Approach with MATLAB*, SpringerBriefs Control Autom. Robot., Springer, New York, 2014, https://doi.org/10.1007/978-1-4939-2107-2.

[11] H. Brezis, *Functional Analysis, Sobolev Spaces and Partial Differential Equations*, Universitext, Springer, New York, 2011, https://doi.org/10.1007/978-0-387-70914-7.

[12] F. Chatelin, *The spectral approximation of linear operators with applications to the computation of eigenelements of differential and integral operators*, SIAM Rev., 23 (1981), pp. 495–522, https://doi.org/10.1137/1023099.

[13] C. W. Clenshaw and A. R. Curtis, *A method for numerical integration on an automatic computer*, Numer. Math. (Heidelb), 2 (1960), pp. 197–205, https://doi.org/10.1007/bf01386223.

[14] P. J. Davis and P. Rabinowitz, *Methods of Numerical Integration*, Comp. Sci. Appl. Math., Academic Press, New York, 2nd ed., 2007.

[15] S. De Reggi, F. Scarabel, and R. Vermiglio, *Approximating reproduction numbers: a general numerical method for age-structured models*, Math. Biosci. Eng., 21 (2024), pp. 5360–5393, https://doi.org/10.3934/mbe.2024236.

[16] O. Diekmann, J. A. P. Heesterbeek, and J. A. J. Metz, *On the definition and the computation of the basic reproduction ratio R_0 in models for infectious diseases in heterogeneous populations*, J. Math. Biol., 28 (1990), pp. 365–382, https://doi.org/10.1007/bf00178324.

[17] O. Diekmann, J. A. P. Heesterbeek, and M. G. Roberts, *The construction of next-generation matrices for compartmental epidemic models*, J. R. Soc. Interface, 7 (2010), pp. 873–885, https://doi.org/10.1098/rsif.2009.0386.

[18] O. Diekmann, F. Scarabel, and R. Vermiglio, *Pseudospectral discretization of delay differential equations in sun-star formulation: Results and conjectures*, Discr. Cont. Dyn. Syst. Ser. S, 13 (2020), pp. 2575–2602, https://doi.org/10.3934/dcdss.2020196.

[19] W. J. Edmunds, G. F. Medley, and D. J. Nokes, *The transmission dynamics and control of hepatitis B virus in the Gambia*, Stat. Med., 15 (1996), pp. 2215–2233, https://doi.org/10.1002/(SICI)1097-0258(19961030)15:20⟨2215::AID-SIM369⟩3.0.CO;2-2.

[20] K. J. Engel and R. Nagel, *One-Parameter Semigroups for Linear Evolution Equations*, vol. 194 of Grad. Texts in Math., Springer, 2000, https://doi.org/10.1007/b97696.

[21] B. T. Grenfell and R. M. Anderson, *The estimation of age-related rates of infection from*

case notifications and serological data, Epidemiol. Infect., 95 (1985), pp. 419–436, https://doi.org/10.1017/s0022172400062859.

[22] W. Guo, M. Ye, X. Li, A. Meyer-Baese, and Q. Zhang, *A theta-scheme approximation of basic reproduction number for an age-structured epidemic system in a finite horizon*, Math. Biosci. Eng., 16 (2019), pp. 4107–4121, https://doi.org/10.3934/mbe.2019204.

[23] J. A. P. Heesterbeek and M. G. Roberts, *The type-reproduction number T in models for infectious disease control*, Math. Biosci., 206 (2007), pp. 3–10, https://doi.org/10.1016/j.mbs.2004.10.013.

[24] M. Iannelli, *Mathematical Theory of Age-Structured Population Dynamics*, Giardini Editori e Stampatori, Pisa, 1995.

[25] H. Inaba, *Mathematical analysis of an age-structured SIR epidemic model with vertical transmission*, Discr. Cont. Dyn. Syst. Ser. B, 6 (2006), pp. 69–96, https://doi.org/10.3934/dcdsb.2006.6.69.

[26] H. Inaba, *On the definition and the computation of the type-reproduction number T for structured populations in heterogeneous environments*, J. Math. Biol., 66 (2013), pp. 1065–1097, https://doi.org/10.1007/s00285-012-0522-0.

[27] H. Inaba, *Age-Structured Population Dynamics in Demography and Epidemiology*, Springer, Singapore, 2017, https://doi.org/10.1007/978-981-10-0188-8.

[28] M. G. Krein and M. A. Rutman, *Linear operators leaving invariant a cone in a Banach space*, Uspekhi Mat. Nauk., 3 (1948), pp. 3–95.

[29] R. Kress, *Linear Integral Equations*, vol. 82 of Appl. Math. Sci., Springer-Verlag, Berlin, Heidelberg, 1989, https://doi.org/10.1007/978-1-4614-9593-2.

[30] V. I. Krylov, *Convergence of algebraic interpolation with respect to the roots of Chebyshev's polynomial for absolutely continuous functions and functions of bounded variation*, Dokl. Akad. Nauk SSSR, 107 (1956), pp. 362–365.

[31] T. Kuniya, *Numerical approximation of the basic reproduction number for a class of age-structured epidemic models*, Appl. Math. Lett., 73 (2017), pp. 106–112, https://doi.org/10.1016/j.aml.2017.04.031.

[32] M. A. Lewis, Z. Shuai, and P. van den Driessche, *A general theory for target reproduction numbers with applications to ecology and epidemiology*, J. Math. Biol., 78 (2019), pp. 2317–2339, https://doi.org/10.1007/s00285-019-01345-4.

[33] P. Liang, J. Zu, and G. Zhuang, *A literature review of mathematical models of hepatitis B virus transmission applied to immunization strategies from 1994 to 2015*, J. Epidemiol., 28 (2018), pp. 221–229, https://doi.org/10.2188/jea.je20160203.

[34] G. Mastroianni and G. V. Milovanović, *Interpolation Processes: Basic Theory and Applications*, Springer Monogr. Math., Springer, Berlin, 2008, https://doi.org/10.1007/978-3-540-68349-0.

[35] J. Prestin, *Lagrange interpolation for functions of bounded variation*, Acta Math. Hungar., 62 (1993), pp. 1–13, https://doi.org/10.1007/BF01874212.

[36] J. Ripoll and J. Font, *Numerical approach to an age-structured Lotka–Volterra model*, Math. Biosci. Eng., 20 (2023), pp. 15603–15622, https://doi.org/10.3934/mbe.2023696.

[37] T. J. Rivlin, *An Introduction to the Approximation of Functions*, Dover Publications, New York, 1981.

[38] F. Scarabel and R. Vermiglio, *Equations with infinite delay: pseudospectral discretization for numerical stability and bifurcation in an abstract framework*, SIAM J. Numer. Anal., 62 (2024), pp. 1736–1758, https://doi.org/10.1137/23M1581133.

[39] J. Szabados and A. Varma, *On mean convergence of derivatives of Lagrange interpolation*, in A Tribute to Paul Erdös, Ed. by A. Baker, B. Bollobás, and A. Hajnal. Cambridge University Press, Cambridge, 1990, pp. 397–407.

[40] H. R. Thieme, *Spectral bound and reproduction number for infinite-dimensional population structure and time heterogeneity*, SIAM J. Appl. Math., 70 (2009), pp. 188–211, https://doi.org/10.1137/080732870.

[41] L. N. Trefethen, *Spectral Methods in MATLAB*, Software Environ. Tools, SIAM, Philadelphia, 2000, https://doi.org/10.1137/1.9780898719598.

[42] L. N. Trefethen, *Is Gauss quadrature better than Clenshaw–Curtis?*, SIAM Rev., 50 (2008), pp. 67–87, https://doi.org/10.1137/060659831.

[43] L. N. Trefethen, *Approximation Theory and Approximation Practice*, SIAM, Philadelphia, 2013.

[44] P. Van den Driessche, *Reproduction numbers of infectious disease models*, Infect. Dis. Model., 2 (2017), pp. 288–303, https://doi.org/10.1016/j.idm.2017.06.002.

[45] P. Van den Driessche and J. Watmough, *Reproduction numbers and sub-threshold endemic equilibria for compartmental models of disease transmission*, Math. Biosci., 180 (2002),

pp. 29–48, https://doi.org/10.1016/s0025-5564(02)00108-6.

[46] G. Webb, *Theory of Nonlinear Age-Dependent Population Dynamics*, vol. 89 of Monogr. Textb. Pure Appl. Math., Marcel Dekker, New York, 1985.

[47] J. Williams, D. Nokes, G. Medley, and R. Anderson, *The transmission dynamics of hepatitis B in the UK: a mathematical model for evaluating costs and effectiveness of immunization programmes*, Epidemiol. Infect., 116 (1996), pp. 71–89, https://doi.org/10.1017/s0950268800058970.

[48] K. Xu, *The Chebyshev points of the first kind*, Appl. Numer. Math., 102 (2016), pp. 17–30, https://doi.org/10.1016/j.apnum.2015.12.002.

[49] S. Zhao, Z. Xu, and Y. Lu, *A mathematical model of hepatitis B virus transmission and its application for vaccination strategy in China*, Int. J. Epidemiol., 29 (2000), pp. 744–752, https://doi.org/10.1093/ije/29.4.744.

[50] L. Zou, S. Ruan, and W. Zhang, *An age-structured model for the transmission dynamics of hepatitis B*, SIAM J. Appl. Math., 70 (2010), pp. 3121–3139, https://doi.org/10.1137/090777645.